Spreading and fingering in spin coating

Kristi E. Holloway,[1] Piotr Habdas,[2] Naeim Semsarillar,[3] Kim Burfitt,[1] and John R. de Bruyn[1,4]
[1]*Department of Physics and Physical Oceanography, Memorial University of Newfoundland, St. John's, Newfoundland, Canada A1B 3X7*
[2]*Department of Physics, Saint Joseph's University, Philadelphia, Pennsylvania 19131-1395, USA*
[3]*Department of Computer Science, Stanford University, Stanford, California 94305-9025, USA*
[4]*Department of Physics and Astronomy, The University of Western Ontario, London, Ontario, Canada N6A 3K7*
(Received 19 July 2006; revised manuscript received 30 January 2007; published 25 April 2007)

We study the spreading and fingering of drops of silicone oil on a rotating substrate for a range of rotation speeds and drop volumes. The spreading of the drop prior to the onset of fingering is found to follow the theoretically predicted time dependence, but with a large shift in time scale. For the full range of experimental parameters studied, the contact line becomes unstable and fingers develop when the radius of the drop becomes sufficiently large. We study the growth of perturbations around the perimeter of the drop and find the growth rate of the most unstable mode to agree well with the predictions of lubrication theory. The number of fingers which form around the perimeter of the drop is found to be a function of both rotation speed and drop volume, and is also in excellent agreement with theoretical predictions.

DOI: 10.1103/PhysRevE.75.046308 PACS number(s): 47.55.nd, 47.54.−r, 47.15.gm

I. INTRODUCTION

Spin coating is a process whereby a volume of fluid spreads on a rotating substrate due to the action of a centrifugal force. Spin coating is used industrially to form thin, uniform coating films in, for example, the manufacture of CDs and flat-screen televisions and in microlithography. A drop of Newtonian fluid positioned on the axis of rotation of a spinning substrate flattens in the middle and forms a capillary ridge around its perimeter as it spreads radially. The capillary ridge can become unstable, leading to the development of fingers at the liquid-substrate contact line [1–3]. This in turn can lead to nonuniform coating of the substrate. Similar contact-line instabilities are observed in thin-film flows down an inclined plane [4–11] and in film flows driven by surface tension gradients [12,13].

Several previous experimental studies of the fingering instability in spin coating have been carried out. Melo *et al.* [2] studied fingering for a range of viscosities, rotation speeds, and fluid volumes using silicone oil. Homsy and co-workers [3,14] studied spin coating in both Newtonian and non-Newtonian fluids. Togashi *et al.* [15] performed spin coating experiments for two Newtonian fluids and derived an analytical expression for the drop radius at which fingering appeared. Other workers have extended the range of rotation speeds [16] and volumes [17] studied. Features of the flow investigated in these experiments include the spreading of the drop prior to fingering, the evolution of the drop profile, the critical radius at which the instability occurs, the number of fingers which formed at the instability, and the growth rates of the fingers.

The spreading of the fluid drop prior to fingering has also been studied theoretically [1–3,18,19], beginning with the early work of Emslie *et al.* [1], who solved the equation for a cylindrical volume of fluid spreading under the action of a centrifugal force using the method of characteristics and showed that the drop radius r should evolve with time t as

$$r(t) = \left(1 + \frac{4}{3}t\right)^{1/4}. \tag{1}$$

Here r is given in units of r_0, the initial radius of the drop, and t in units of the time scale for flow in the region near the contact line, $t_0 = \eta/h_0^2\rho\omega^2$ [3]. η is the viscosity of the fluid and ρ its density, ω the angular frequency of the spinning substrate, and h_0 the initial height of the drop. In deriving Eq. (1) it was assumed that the drop remains cylindrical and that its volume is constant. Wilson *et al.* also studied the spreading of a fluid drop prior to the onset of the fingering instability [18]. They found analytic solutions for $r(t)$ when the surface tension $\gamma=0$ and in the low-γ limit, and studied the problem numerically for finite γ. Their finite-γ solution agreed with the experimental data of Fraysse and Homsy [3] while the analytic solution in the asymptotic limit described the behavior of $r(t)$ qualitatively but not quantitatively.

Once the radius of the fluid drop becomes large enough, the contact line becomes unstable and fingers appear. This instability has been treated theoretically in the context of lubrication theory. Troian *et al.* [4] studied the linear stability of the contact line for the flow of thin film of fluid down an inclined plane, a situation that is mathematically equivalent to flow under the influence of a centrifugal force. They assumed the presence of a thin precursor film ahead of the contact line to remove contact-line singularities. They showed that the contact line is unstable for wave numbers $q \leqslant 0.9/\ell$, with the fastest-growing mode at $q_m \approx 0.45/\ell$. Here $\ell = H(3\mathrm{Ca})^{-1/3}$ is a characteristic length scale near the contact line. H is the height of the film in the region far from the contact line; for the spin coating problem in the lubrication approximation, $H = (3u_0\eta/\rho\omega^2 r)^{1/2}$ [3]. $\mathrm{Ca} = \eta u_0/\gamma$ is the capillary number. Here u_0 is the flow velocity near the contact line. The dimensionless growth rate of the fastest-growing mode was found to be approximately 0.5, depending weakly on the thickness of the precursor film. This theory has been extended to account for the effects of the normal component of gravity in the inclined plane case [9,10]. Spaid and Homsy [20] studied the stability of the contact line using a slip model and found the results to be independent of the contact-line model. McKinley and co-workers [21–23] studied the linear stability of a drop of fluid spreading due to either a centrifugal force or a jet of air, and Schwartz and Roy [24] have recently developed a mathematical model to study the stability of fluid drops during spin coating.

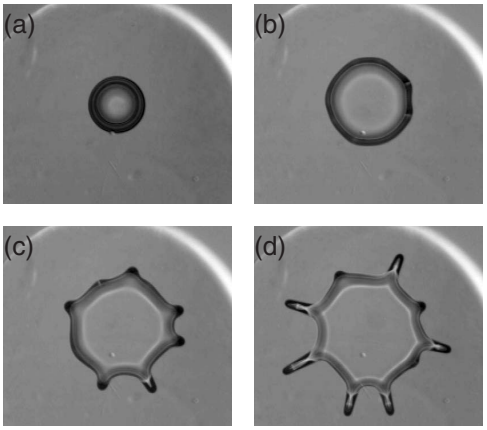

FIG. 1. Shadowgraph images showing the spreading and fingering of a droplet of volume $V=50$ μl. The outer edge of the dark annular region corresponds to the edge of the drop. The angular speed ω of the turntable is 36.8 rad/s. Time $t=0$ corresponds to the start of the rotation. At $t=1.45$ s (a) the drop is circular. At $t=11.45$ s (b) perturbations have started to grow around the perimeter of the drop. In images (c) ($t=21.45$ s) and (d) ($t=31.45$ s) fingers have developed and grown.

Defining r_c as the value of r at which fingers first form at time t_c and assuming the drop volume V is conserved, it is straightforward to show that

$$\ell(t_c) = \left(\frac{\gamma V}{\pi\rho\omega^2 r_c^3}\right)^{1/3}. \tag{2}$$

From this and the wave number of the fastest-growing mode, the number of fingers n that form is found to be [3]

$$n = \frac{\pi}{7} r_c^2 \left(\frac{\pi\rho\omega^2}{\gamma V}\right)^{1/3}. \tag{3}$$

In this paper, we present the results of a systematic study of the fingering instability in spin coating experiments using a relatively low-viscosity silicone oil as the experimental fluid. In Sec. II we describe the experimental apparatus and procedure. In Sec. III the results of our experiments are presented and we compare our results with theoretical predictions and previous work.

II. EXPERIMENT

The experimental apparatus was designed to permit accurate positioning of the fluid drops at the center of the rotating substrate, as well as visualization of the perimeter of the drop as it spreads under the influence of the centrifugal force. The substrate is a circular transparent sapphire plate 10 cm in diameter mounted in a holder that can be rotated by a computer-controlled microstepper motor. The angular velocity ω is varied under computer control in the range 10.5–63 rad/s. The angular acceleration of the plate is fixed at the maximum accessible value of 168 rad/s^2 for all runs discussed in this paper. With this acceleration the plate reached its set angular speed in approximately 0.4 s for the highest ω and in all cases well before the onset of the fingering instability.

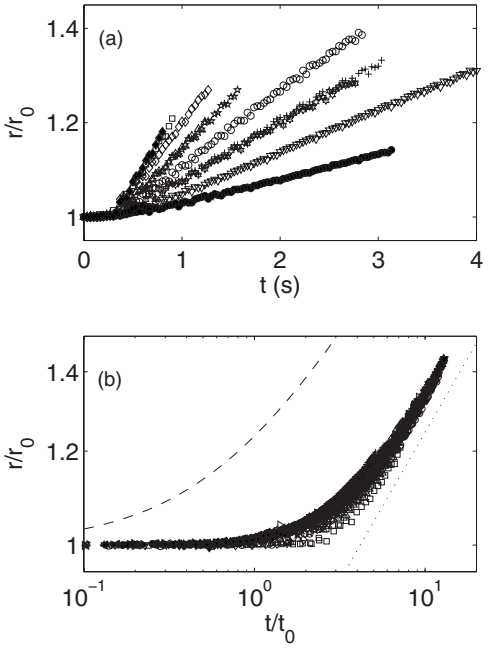

FIG. 2. Spreading of drops of volume $V=100$ μl. (a) shows r/r_0 as a function of time for several drops of the same volume with angular velocities ω equal to 26.3 rad/s (solid circles), 26.6 rad/s (exxes), 31.5 rad/s (solid squares and downward-pointing triangles), 36.7 rad/s (crosses), 36.8 rad/s (six-pointed stars), 42.0 rad/s (open circles), 47.3 rad/s (five-pointed stars and upward-pointing triangles), 52.5 rad/s (open diamonds), and 57.8 rad/s (open squares and solid diamonds). (b) r/r_0 plotted as a function of scaled time, t/t_0, where t_0 is defined in the text. 23 different data sets are shown, covering a range of volumes and angular speeds. The dashed line is the prediction of Eq. (1), and the dotted line is a 1/4-power law plotted for comparison.

The spreading and fingering of the fluid drop was visualized with a shadowgraph optical system [25]. Light from a bright red light-emitting diode is expanded and collimated, then passes through the transparent sapphire plate from below. The shadowgraph image is then focused onto a charge-coupled-device video camera mounted above the apparatus. Contrast in the shadowgraph is due to the deflection of light by thickness variations in the fluid. This method produces high-quality images in which the edges of the fluid drop are clearly defined, as shown in Fig. 1. The video camera is interfaced to a computer which records images of the flow as it progresses at intervals chosen between 0.033 s and 0.1 s. The integration time of the camera is fixed at 10^{-4} s.

The plate is cleaned prior to each run with warm soapy water and then rinsed with clean water and finally with acetone. The plate is mounted in the apparatus and the system is carefully levelled. To place the fluid drop accurately at the center of the plate we used a jig consisting of a metal plate with a small hole machined in its center that could be precisely positioned on the plate holder. Two micrometer-driven translation stages were used to position an arm holding a length of fine plastic tubing above the center of the plate. A syringe pump is used to place a volume of fluid from 50 to 250 μl onto the plate at a rate of 1 ml/min.

The experimental fluid is a Newtonian silicone oil with a viscosity η of 0.053 kg/ms at 20 °C as measured with a

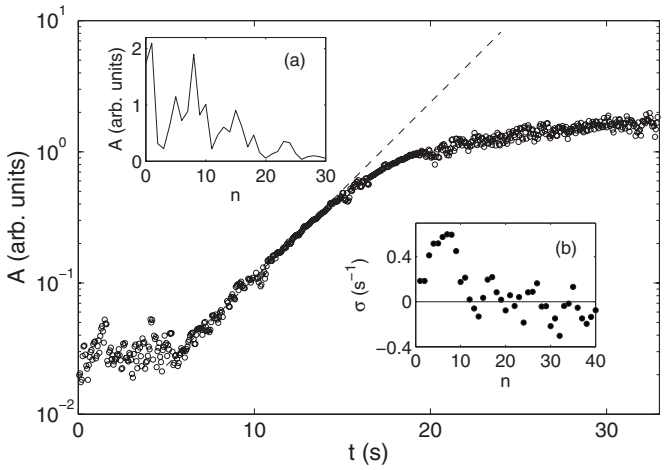

FIG. 3. Inset (a): the Fourier power spectrum of the perimeter of a drop with $V=50$ μl at a time $t=21.45$ s after the start of spinning at $\omega=36.8$ s^{-1}. n is the azimuthal wave number. The large peak at $n=1$ arises because the drop is slightly off-center despite our best efforts to position it accurately. Main figure: the Fourier power of the fastest-growing mode at $n=7$ for the same run as in Fig. 1 and the insets. The dashed line is a fit to an exponential growth law at early times after the onset. Inset (b): the exponential growth rate σ as a function of mode number n. To reduce the noise, the plotted growth rates have been averaged over the modes $n-1$, n, and $n+1$.

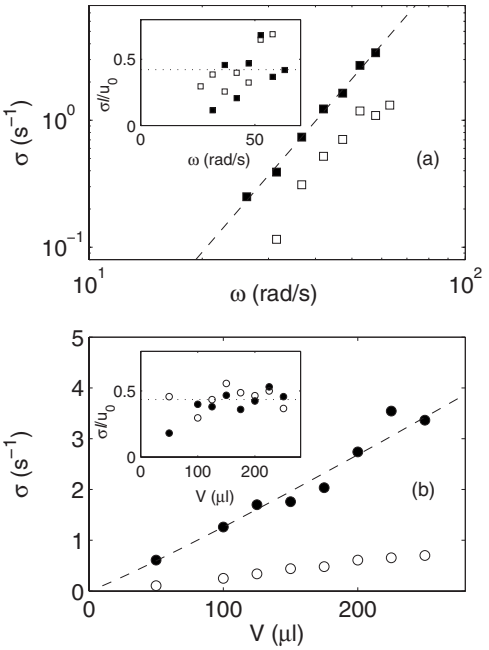

FIG. 4. The growth rate σ of the fingers plotted against ω in (a) and against volume V in (b). In (a) the open squares are for $V=50$ μl, the solid squares for $V=100$ μl, and the dashed line is a power-law fit to the data for $V=100$ μl. In (b), the open circles are for $\omega=26.3$ rad/s, the solid circles for $\omega=42.0$ rad/s, and the dashed line is a straight-line fit to the higher ω data. The insets show the scaled growth rate plotted as a function of ω in (a) and against V in (b). The dotted line is the mean value in each case.

shear rheometer using a cone-and-plate geometry. The density of the oil is $\rho=963$ kg/m^3, and its surface tension is $\gamma=0.0208$ N/m. This silicone oil completely wets the sapphire surface and so has a contact angle of 0. As a result, the drops start to spread immediately once they are deposited on the plate. For our experiments, the drops were allowed to relax for 30 s before the rotation was started. The radius of a 100-μl drop of fluid increases by 0.16 cm during this relaxation time. We take r_0 to be the radius of the fluid drop at the end of this relaxation time, when the motor is turned on.

III. RESULTS AND DISCUSSION

Figure 1 shows a sequence of images from a run with a drop of volume $V=50$ μl and angular speed $\omega=36.8$ rad/s. The contact line is initially circular, as shown in Fig. 1(a). As the drop is rotated it spreads radially under the action of the centrifugal force, initially flattening, then becoming thinner in the middle with a capillary ridge around the perimeter. At some radius r_c the contact line becomes unstable and fingers start to form, as shown in Figs. 1(b) and 1(c). As time progresses these fingers grow, and additional fingers can appear between those that form initially. As seen in Fig. 1, the spacing of the fingers around the perimeter of the drop is approximately uniform. Fingering was observed for the full range of experimental parameters studied here, and the behavior we observe is very similar to that reported in Refs. [2,3].

Figure 2(a) shows the spreading of the drop from $t=0$ to the time t_c at which the fingers begin to form for several runs on drops of the same volume but with different angular speeds. Following an initial period during which the drop radius changes very little, the spreading appears to be linear in time. The spreading rate of the drop depends strongly on ω; analogous experiments for different V at fixed ω show that the spreading rate also depends on V. The slope of the $r(t)/r_0$ plots, which has units of s^{-1}, can be described by power laws: the slope is proportional to $V^{0.73\pm0.05}$ and to $\omega^{2.47\pm0.17}$. Overall we found that $r/r_0=(1.64\pm0.10)\times10^{-7}\omega^{2.47}V^{0.73}t$ in this regime, with ω in rad/s and V in μl. Dimensional analysis can be used to form an inverse time scale given by $V^{3/4}\omega^{5/2}\rho^{3/4}\gamma^{-3/4}$, which has the correct volume and angular velocity dependence, but the theoretical basis for such a time scale, if any, is not clear.

The theory of spin coating derived by Emslie *et al.* [1] predicts that the radius of the spreading drop should be described by Eq. (1). Our data are plotted in this form in Fig. 2(b). The scaled data collapse very well and have a dependence on t/t_0 that is close to the predicted 1/4 power law at large times. On the other hand, our data are systematically shifted to the right of the predicted curve, shown as the dashed line in Fig. 2(b). In contrast, Fraysse and Homsy found a rather poor collapse of their data using this scaling [3], and both they and Melo *et al.* [2] found that the spreading curves at longer times had a logarithmic slope greater than the predicted value of 1/4.

The shift between the theoretical curve and the experimental data can perhaps be explained by the theoretical assumption that the drop is cylindrical in shape, whereas in practice there is a significant, and time-dependent, radial

variation in the height of the drop. The theoretical curve in Fig. 2(b) can be brought closer to the experimental data by a 60% change in the initial radius values, in effect changing the time scale t_0 by the same fraction. This shift is much larger than any experimental uncertainty and seems larger than might be accounted for by the variation in drop shape. Fraysse and Homsy [3] found a similar result in their experiments, but required a shift in r_0 of only 10%–15% to bring theory and experiment into agreement. This persistent discrepancy between theory and experiment suggests that the scalings used in the derivation of Eq. (1) are inappropriate [3]. ω increases from zero to its set value over part of the initial period of slow spreading, although in all cases it is constant by the time the spreading rate starts to increase. This means that t_0 is in fact changing over the early part of the experiment and may account in part for the discrepancy between experiment and theory.

To study the fingering instability that develops after the period of uniform spreading, we analyze the experimental images by taking a Fourier transform of the function $r(\theta)$ describing the perimeter of the drop to give the Fourier power spectrum as a function of angular wave number n [3,26,27]. Here θ is the angular coordinate about the axis of rotation. n indicates the number of periods of the mode as θ is varied by 2π radians—that is, the number of maxima around the perimeter of the drop. A typical power spectrum is shown in Fig. 3 [inset (a)]. By analyzing a time series of images in this way, we obtain the amplitude of the modes as a function of time t. The amplitude of the $n=7$ mode from the same run used in Fig. 1 and in the insets to Fig. 3 is plotted against time in Fig. 3. The amplitude is initially constant, then starts to grow exponentially at a time $t_c=5.9$ s. At later times the growth slows and the amplitude approaches a

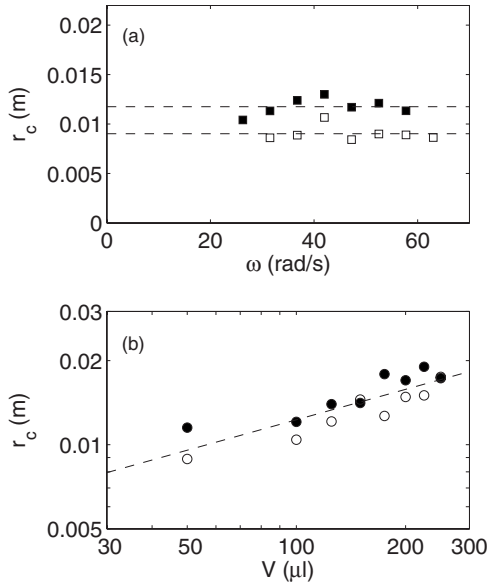

FIG. 5. The critical radius r_c as a function of ω (a) and as a function of V (b). In (a), the open squares are for $V=50$ μl and solid squares for $V=100$ μl. In (b), the open circles are for $\omega=26.3$ rad/s and solid circles for $\omega=42.0$ rad/s. The dashed lines in (a) show the average values of the two data sets, and in (b) the dashed line is a fit to all of the data.

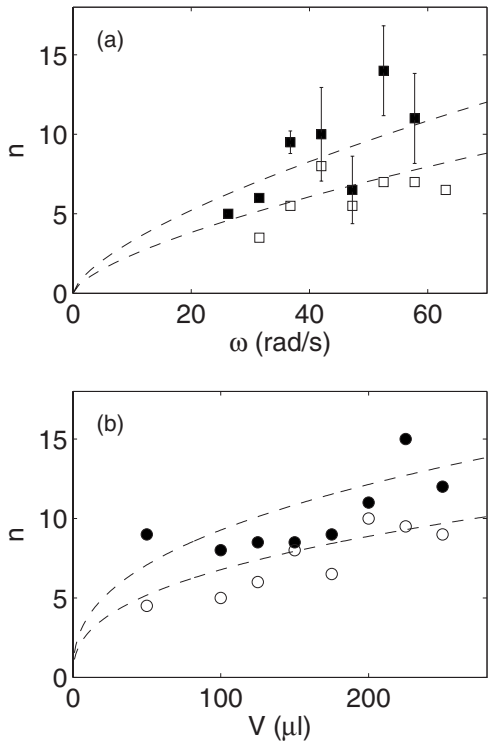

FIG. 6. (a) n as a function of ω for $V=50$ μl (open squares) and $V=100$ μl (solid squares). Error bars are shown for one data set. The dashed lines are the predictions of the theoretical expression, Eq. (3), using the fits to the data for r_c shown in Fig. 5. There are no free parameters. (b) The number of fingers n as a function of V for two values of the rotation speed. The open circles are for $\omega=26.3$ rad/s and the solid circles for $\omega=42.0$ rad/s. The dashed lines are again the predictions of Eq. (3), using the fits to the experimental data for the critical radius r_c shown in Fig. 5.

constant. The initial exponential growth rate σ is calculated for each n from a fit to the amplitude data over the range of exponential growth. Figure 3 [inset (b)] shows that σ is positive for small n and becomes negative at high n, as expected. In this particular case σ is a maximum for $n=7$ which corresponds to the number of fingers seen to develop in Fig. 1 at early times.

σ increases with both angular speed and volume. σ is plotted as a function of V in Fig. 4. The volume dependence is linear, while the dependence on ω is well described by a power law with an exponent of 3.41 ± 0.01. Combining these, our results give $\sigma=(3.4\pm0.1)\times10^{-8}V\omega^{3.41}$, where σ has units of s^{-1}, V in μl, and ω in rad/s. The dimensionless growth rate $\sigma\ell/u_0$, where u_0 is the radial speed of the perimeter of the drop at $t=t_c$, is shown in the inset to Fig. 4. The mean value of $\sigma\ell/u_0=0.43\pm0.16$ is in excellent agreement with the theoretical predictions of Ref. [4] and with previous experiments on spin coating [3].

In the case of a sheet of fluid flowing down an incline, the downslope spreading is driven by the in-plane component of gravity, but the normal component of gravity has a significant influence on both the wavelength and the growth rate of the fingering instability [9]. For our spin coating experiments, gravity always acts perpendicular to the centrifugal force which drives the spreading, and itself drives flattening

and spreading of the drop before the substrate starts to rotate. The ratio of the gravitational force to the centrifugal force in our experiments is in the range $0.26 < g/\omega^2 r < 1.7$, being less than 1 in most cases. The corresponding ratio for the inclined plane experiments is normally greater than 1 and is greater than 10 for low inclination angles. Thus while one would expect some deviations from the predictions of Ref. [4] due to gravity, they are unlikely to be large.

The radius r_c at which fingers begin to form is plotted against the drop volume and angular speed in Fig. 5. For a given V, r_c is independent of ω over the range of angular speeds studied, having average values of 0.0090 ± 0.0008 m for $V=50$ μl and 0.0118 ± 0.0009 m for $V=100$ μl. r_c increases with V as $V^{0.36 \pm 0.02}$, consistent with the $V^{1/3}$ dependence one might expect from simple dimensional considerations.

The number of fingers, n, that form at the instability is shown as a function of volume for two values of ω in Fig. 6(a) and as a function of speed for $V=50$ and 100 μl in Fig. 6(b). Our results show a systematic increase in n with both ω and V over the range covered by our experiments. In fact our experimental results are in quantitative agreement with Eq. (3): the dashed lines in Figs. 6(a) and 6(b) are the theoretical predictions, calculated using the fits to our measured values of r_c described in the previous paragraph. There are no free parameters, and, within the scatter of our data, the agreement is excellent. In contrast, previous work has suggested that n was independent of both ω and V [2,3], perhaps because the change in n was too small to be detected over the range of experimental parameters studied previously. This led Fraysse and Homsy [3] to assume a particular functional form for r_c in order that the ω and V dependence in Eq. (3) would cancel out. Our measurements of r_c, shown in Fig. 5, do *not* follow the form assumed in Ref. [3], however.

IV. CONCLUSION

We have studied the spin coating of a drop of silicone oil for a range of volumes and rotation speeds. The drop spreads under the influence of the centrifugal force in qualitative agreement with theoretical predictions, but with a substantial shift in scaled time, suggesting that the scaling used in the theoretical expression is inappropriate. Once the radius of the spreading drop became large enough, a fingering instability developed at the contact line. The number of fingers increased with both angular speed and drop volume while the scaled growth rate of the fingers was constant, both in quantitative agreement with theoretical predictions.

ACKNOWLEDGMENTS

This research was supported by the Natural Sciences and Engineering Council of Canada. We thank N. P. Chafe and A. Walsh for useful discussions.

[1] A. G. Emslie, F. T. Bonner, and L. G. Peck, J. Appl. Phys. **29**, 858 (1957).
[2] F. Melo, J. F. Joanny, and S. Fauve, Phys. Rev. Lett. **63**, 1958 (1989).
[3] N. Fraysse and G. M. Homsy, Phys. Fluids **6**, 1491 (1994).
[4] S. M. Troian, E. Herbolzheimer, S. A. Safran, and J. F. Joanny, Europhys. Lett. **10**, 25 (1989).
[5] H. E. Huppert, Nature (London) **300**, 427 (1982).
[6] L. W. Schwartz, Phys. Fluids A **1**, 443 (1989).
[7] J. R. de Bruyn, Phys. Rev. A **46**, R4500 (1992).
[8] J. M. Jerrett and J. R. de Bruyn, Phys. Fluids A **4**, 234 (1992).
[9] M. P. Brenner, Phys. Rev. E **47**, 4597 (1993).
[10] A. L. Bertozzi and M. P. Brenner, Phys. Fluids **9**, 530 (1997).
[11] J. R. de Bruyn, P. Habdas, and S. Kim, Phys. Rev. E **66**, 031504 (2002).
[12] S. M. Troian, X. L. Wu, and S. A. Safran, Phys. Rev. Lett. **62**, 1496 (1989).
[13] S. M. Troian, E. Herbolzheimer, and S. A. Safran, Phys. Rev. Lett. **65**, 333 (1990).
[14] M. A. Spaid and G. M. Homsy, Phys. Fluids **9**, 823 (1997).
[15] S. Togashi, T. Ohta, and H. Azuma, J. Chem. Eng. Jpn. **34**, 1402 (2001).
[16] M.-W. Wang and F.-C. Chou, J. Electrochem. Soc. **148**, 283 (2001).
[17] I. Veretennikov, A. Agarwal, A. Indeikina, and H.-C. Chang, J. Colloid Interface Sci. **215**, 425 (1999).
[18] S. K. Wilson, R. Hunt, and B. R. Duffy, J. Fluid Mech. **413**, 65 (2000).
[19] Y. D. Shikhmurzaev, Phys. Fluids **9**, 266 (1997).
[20] M. A. Spaid and G. M. Homsy, Phys. Fluids **8**, 460 (1996).
[21] I. S. McKinley, S. K. Wilson, and B. R. Duffy, Phys. Fluids **11**, 30 (1999).
[22] I. S. McKinley and S. K. Wilson, Phys. Fluids **13**, 872 (2001).
[23] I. S. McKinley and S. K. Wilson, Phys. Fluids **14**, 133 (2002).
[24] L. W. Schwartz and R. V. Roy, Phys. Fluids **16**, 569 (2004).
[25] W. Merzkirch, *Flow Visualization* (Academic, Orlando, 1987).
[26] K. E. Holloway and J. R. de Bruyn, Can. J. Phys. **83**, 551 (2005).
[27] K. E. Holloway and J. R. de Bruyn, Can. J. Phys. **84**, 273 (2006).